Dalton Transactions

ROYAL SOCIETY OF CHEMISTRY

PAPER

View Article Online
View Journal | View Issue

Cite this: *Dalton Trans.*, 2026, **55**, 885

Minimal liquid-assisted method for synthesis of ammonium, sodium, and potassium intercalated zirconium hydrogen phosphate: the effect of the cation used on the formation of an α- or γ-structure

Klára Melánová, *[a] Ludvík Beneš, [a] Rokas Lemežis,[b] Vytautas Klimavičius[b] and Jan Smolík[a]

Zirconium hydrogen phosphates intercalated with ammonium, sodium, and potassium cations were successfully synthesized *via* a minimal liquid-assisted approach, involving the grinding of a zirconium precursor with the corresponding metal dihydrogen phosphate, followed by thermal treatment. The resulting crystalline phase—either α- or γ-type zirconium phosphate—was found to depend on both the intercalating cation and the zirconium source. Potassium dihydrogen phosphate consistently yielded compounds with α-structure, whereas ammonium and sodium dihydrogen phosphates led to either α- or γ-phases, depending on the dihydrogen phosphate and phosphoric acid molar ratio in the starting reaction mixture, and also the zirconium source employed. An increase in the P/Zr molar ratio and reaction temperature enhanced product crystallinity without altering phase composition. The presence of α- or γ-type intercalates was confirmed through hydrochloric acid treatment, which selectively yielded α- or γ-zirconium phosphate, and further validated through solid-state ^{31}P NMR spectroscopy.

Received 23rd October 2025,
Accepted 11th December 2025

DOI: 10.1039/d5dt02548f

rsc.li/dalton

Introduction

Layered zirconium phosphates (ZrP) are 2D materials which are promising functional materials for applications as catalysis, optical and electronic materials, drug delivery or battery materials.[1–3] Various chemical methods, such as refluxing, hydrothermal, sol–gel, microemulsion, microwave, as well as minimal solvent method, can be used for the synthesis of both amorphous and crystalline phases of ZrP.[1,4,5] All these synthetic strategies involve the addition of phosphate to a solution of zirconium(IV) salt, resulting in precipitation of ZrP. The choice of preparation method and reaction conditions strongly influences not only the degree of crystallinity, but also the shape and size of the particles. The reflux method was first reported by Clearfield *et al.*,[6] who obtained crystalline α-ZrP by refluxing an amorphous ZrP in concentrated H_3PO_4. The crystallinity of the product increased upon increasing acid concentration and refluxing time. Later, in 2000, it was found that crystalline ZrP could be obtained simply by slowly adding excess H_3PO_4 to an acidified solution of zirconium oxychloride at room temperature, followed by washing of the precipitate with a diluted solution of H_3PO_4.[7] It was shown that originally precipitated crystalline α-ZrP became amorphous during washing with distilled water. To obtain a highly crystalline product, the precipitation of Zr(IV) ions is performed in the presence of complexing agents such as HF,[8] oxalic acid[9] or formamide.[10] A hydrothermal method was used to better control the morphology and crystallinity of the resulting α-ZrP.[11,12] Sol–gel synthesis, based on the addition of concentrated phosphoric acid to a solution of zirconium propoxide in 1-propanol, leads to an amorphous or semicrystalline material depending on aging time.[13]

In order to avoid the excess use of H_3PO_4 and complexing agents, solid state methods using various alkali metal phosphates were developed.[14,15] Minimal liquid approach, in which reagents are mixed in their as-obtained state and concentration, was used for the synthesis α-ZrP.[16] $ZrOCl_2{\cdot}8H_2O$ was mixed with concentrated orthophosphoric acid (P/Zr = 2 or 3) and heated at 25–120 °C for 24 h. Larger crystals were obtained at a higher P/Zr ratio and the crystallinity of the sample increased with increasing reaction temperature. If a small amount of fluoride ions was added into the reaction mixture,

[a]*Center of Materials and Nanotechnologies, Faculty of Chemical Technology University of Pardubice, Studentská 95, 532 10 Pardubice, Czech Republic. E-mail: klara.melanova@upce.cz*
[b]*Institute of Chemical Physics, Vilnius University, Saulėtekio ave. 3, LT-10257 Vilnius, Lithuania*

the highly crystalline product was obtained and its morphology changed from platelets to rod shape particles with increasing F/Zr ratio. Layered α-disodium zirconium phosphate was synthesized by one-pot reaction of zirconium oxychloride octahydrate and with Na_2HPO_4 in the presence of a small amount of NaF.[17] Similarly, α-$Zr(NH_4PO_4)_2{\cdot}2H_2O$ was prepared using $ZrOCl_2{\cdot}8H_2O$ and $(NH_4)_2HPO_4$.[18] A highly crystalline γ-ZrP can be obtained using NaH_2PO_4 followed by treatment with diluted hydrochloric acid.[19]

In order to move the field further, in this work we have focused in the reactions of various zirconium sources with ammonium, sodium, and potassium dihydrogen phosphates. The influence of reaction conditions (cation type, zirconium source, P/Zr molar ratio, reaction temperature) on fine details of the end material was studied by means of PXRD, EDX and solid-state NMR.

Experimental

Synthetic procedures

Sodium, potassium and ammonium dihydrogen phosphates, zirconium(IV) oxychloride octahydrate, zirconium(IV) oxynitrate hydrate and zirconium(IV) propoxide were obtained from Merck s.r.o., Czech Republic. Zirconium(IV) sulfate tetrahydrate was obtained from Fisher Scientific, spol. s.r.o., Czech Republic. A well-crystallized γ-$NH_4Zr(PO_4)(HPO_4)$ and γ-$Zr(PO_4)(H_2PO_4){\cdot}2H_2O$ was obtained according to Poojary *et al.*[20]

To monitor the influence of the Zr/P molar ratio and reaction temperature, zirconium oxychloride octahydrate (0.161 g, 0.5 mmol) was mixed with an appropriate amount of the corresponding dihydrogen phosphate (1, 1.5, 2, 2.5, and 3 mmol). The samples were ground together in an agate mortar with the addition of 2–3 drops of distilled water to form a thick paste. After 5 minutes of grinding, the paste was transferred to a closed Teflon container and heated at a temperature of 120, 140, 160, or 180 °C for 48 hours. Heated samples were washed three times with distilled water.

To monitor the effect of the zirconia source used, zirconium oxychloride octahydrate, zirconium(IV) oxynitrate hydrate, zirconium(IV) propoxide, or zirconium(IV) sulfate tetrahydrate (0.5 mmol) was mixed with the corresponding dihydrogen phosphate (2 mmol). The ground samples were heated at 120 °C for 48 hours. Heated samples were washed three times with distilled water.

To study the influence of metal/hydrogen ratio, reaction mixtures according to the equation:

$$ZrOCl_2 + xMH_2PO_4 + (4-x)H_3PO_4 \rightarrow M_yH_{(2-y)}Zr(PO_4)_2 \cdot nH_2O$$

were prepared by mixing zirconium oxychloride, metal dihydrogen phosphate and phosphoric acid in corresponding ratios and the mixtures were treated as given above. The same mixtures were prepared using zirconium propoxide.

Highly crystalline comparative samples were prepared by shaking γ-ZrP, (0.5 g) with an excess of Na_2CO_3, K_2CO_3 or NH_4Cl dissolved in a mixture of water and ethanol (25 mL + 5 mL) at room temperature for three days. The solid products were collected by centrifugation, three times washed with distilled water and dried in air. Their compositions are given in the Table S1 of the SI.

Characterization

Powder X-ray diffraction data (Cu Kα, λ = 1.5418 Å) of powdered sample was collected on a Diffractometer D8 ADVANCE. DAVINCI (Bruker AXS, Germany) with Bragg–Brentano θ–θ goniometer (radius 280 mm) equipped with a LynxEye XE-T detector. The generator operated at 40 kV and 30 mA. The diffraction angles were measured at room temperature from 2 to 50° (2θ) in 0.01° steps with a counting time of 1 s per step (total time 85 min). The PDF5+ database[21] was used to identify crystalline phases. The powder patterns of selected sodium and potassium intercalates was indexed using DICVOL91 program from the CRYSFIRE software package.[22] The lattice parameters were refined by Le Bail's method using FullProf program.[23]

Scanning electron microscopy (SEM) and energy-dispersive X-ray analysis (EDX) was done using an electron scanning microscope JEOL JSM-5500LV equipped with an energy-dispersive X-ray microanalyzer IXRF Systems (detector GRESHAM Sirius 10). The accelerating voltage of the primary electron beam was 20 kV. EDX was measured from five different sample locations, the results reported are the average of these measurements. The content of nitrogen in ammonium intercalated ZrP was determined using organic elemental analysis.

The thermogravimetric analysis was done using a home-made apparatus constructed of a computer-controlled oven and a Sartorius BP210 S balance. The measurements were carried out in air between 30 and 960 °C at a heating rate of 5 °C min^{-1}.

Solid-state NMR experiments were carried out at 9.4 T on a Bruker Avance III HD 400 NMR spectrometer operating at 400.2, 162.0 and 105.8 MHz for ^1H, ^{31}P and ^{23}Na, respectively, using a 4 mm double resonance CP MAS probe and 4 mm zirconia rotors. The temperature was stabilized at 298 K and the MAS rate was set to 10 kHz. For ^{31}P MAS measurements, a saturation recovery pulse sequence was used. The saturation pulse train consisted of 20 π/2 pulses followed by 500 s delay. The π/2 excitation pulse was equal to 2.5 μs, 2 scans were accumulated and the spinal64 ^1H decoupling scheme was used. For ^{31}P–^{31}P 1Q–2Q experiments, a cross polarization-based pulse sequence was used, which employs a BABA (back-to-back) 2 rotor periods recoupling scheme. The ^{31}P π/2 excitation pulse was equal to 2.5 μs, the repetition delay was set to 10 s and 32 scans per 64 increments were accumulated. ^{23}Na MAS NMR spectra were measured using a Hahn-echo pulse sequence, the π/2 pulse was set to 2.7 μs, the relaxation delay was 5 s and 256 scans were accumulated. For ^{23}Na MQMAS, measurements 480 scans for 32 increments were accumulated, the excitation, conversion and selective pulses were set to 6.4 μs, 2.0 μs and 85 μs, respectively. ^{31}P spectra were referenced to 85% H_3PO_4 using ADP (ammonium dihydrogen phos-

phate, $NH_4H_2PO_4$, δ (^{31}P) = 0.8 ppm) as external standard. ^{23}Na spectra were referenced using NaCl (δ (^{23}Na) = 0 ppm).

Results and discussion

Influence of P/Zr molar ratio and temperature

Intercalates of ZrP with alkali metals and ammonium were prepared at five different P/Zr molar ratios (2, 3, 4, 5 and 6) and at four temperatures – 120, 140, 160, and 180 °C using the most common zirconium source – zirconium oxychloride and corresponding dihydrogen phosphate. Powder X-ray diffraction (PXRD) patterns of the prepared compounds are shown in Fig. 1 and S1 in SI. For comparison, the powder patterns of the intercalates prepared by ion exchange from γ-ZrP were added.

In the case of ammonium intercalates, a nearly amorphous sample was obtained at the starting molar ratio P/Zr = 2 and 120–160 °C. Crystalline products were formed at P/Zr = 3 or 4, further increasing the P/Zr ratio in the reaction mixture no longer leads to an improvement in crystallinity. The basal spacing of the products is in all cases about 11.3 Å, which is in agreement with the powder pattern of γ-$H(NH_4)Zr(PO_4)_2$ (JCPDS no. 04-014-2214, marked in red).

SEM images of the ammonium intercalates prepared are presented in Fig. S2 in SI. The intercalate synthesized by ion exchange preserve the morphology of the initial γ-ZrP that is well-developed rods and platelets. In contrast, the intercalates prepared by minimal liquid method consist of agglomerates of particles with a non-specific shape regardless of the P/Zr ratio or temperature used. The change in particle morphology is caused by a change in the relative growth rate in individual crystal directions.[24] Looking at the diffraction patterns of samples prepared by ion exchange and minimal liquid method, there is a clear difference in the ratios of the intensities of the individual diffraction lines. In the case of the samples prepared by minimal liquid method, the most intense line of is (011) at 15.5° and the intensity of the (020) line at 26.9° is in most cases comparable to or greater than that of the (001) line at 11.3°, while the intensities of the lines ion-exchanged samples decrease in the order (001) > (011) > (020). This suggests that the growth rate along the *c* axis is comparable to growth rate in the layer plane in the samples prepared by minimal liquid method, which affects particle morphology.

Only a poorly crystalline sodium compound was obtained at the starting molar ratio P/Zr = 2 and 120 and 140 °C (see Fig. 2 and S3 in SI), while highly crystalline $NaZr_2(PO_4)_2$ is formed at 160 °C. Products with higher crystallinity were formed at higher starting ratios at all temperatures and at P/Zr = 2 at 180 °C. The basal spacing of the products ranges between 10.04 and 11.70 Å, which indicates the formation of γ-modification. The difference in the basal spacing is connected to the water content in the interlayer space of the intercalate. The basal spacing value of 11.60 Å given in the PDF5+ database for $Zr(PO_4)(NaHPO_4)\cdot 2.5H_2O$ (JCPDS no. 00-032-1217) is the same as the value measured for the intercalate obtained by ion exchange and very close to values for the phases with the higher basal spacing obtained by the minimalistic liquid-assisted method. The phases with lower basal spacing of about 10.3 Å correspond probably to anhydrous $Zr(PO_4)(NaHPO_4)$.[19] As the data given in the PDF5+ database are marked as low precision and are not indexed, we try to index the diffraction pattern of the Na-intercalate prepared by ionic exchange with a composition $NaHZr(PO_4)(HPO_4)\cdot 1.4H_2O$. It can be indexed in a monoclinic system with lattice parameters a = 11.8439 ± 0.0004 Å, b = 5.3240 ± 0.0002 Å, c = 6.6302 ± 0.0002 Å, β = 102.238 ± 0.005°, see Table S2 and Fig. S4 in the SI.

SEM images of the sodium intercalates prepared are shown in Fig. S5 in SI. Similarly as it was in the case of ammonium,

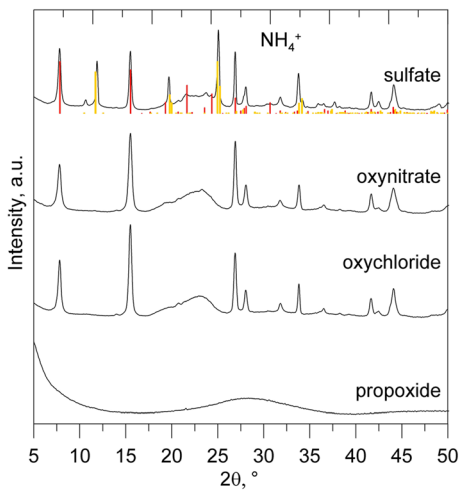

Fig. 1 Powder X-ray diffraction patterns of NH_4 intercalates prepared at various P/Zr ratios and temperatures and by ionic exchange from γ-ZrP. Red lines correspond to γ-$H(NH_4)Zr(PO_4)_2$ (JCPDS no. 00-033-0842).

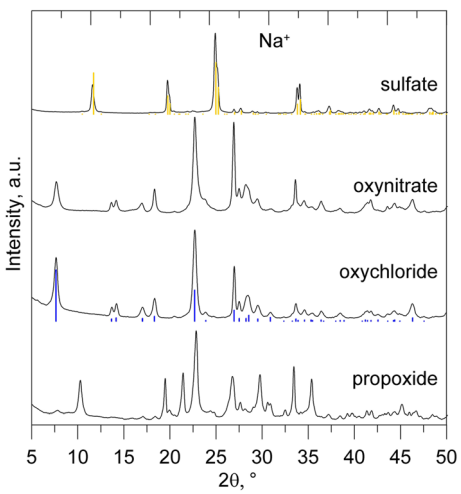

Fig. 2 Powder X-ray diffraction patterns of sodium intercalates prepared at various P/Zr ratios and temperatures and by ionic exchange from γ-ZrP. Blue lines corresponds to indexed pattern of $NaHZr(PO_4)(HPO_4)\cdot 1.4H_2O$, cyan to $Zr(PO_4)(NaHPO_4)\cdot 2.5H_2O$ (JCPDS no. 00-032-1217).

the intercalates prepared by minimal liquid method consist of agglomerates of particles with a non-specific shape.

In contrast to the above-mentioned cations, the reaction of zirconium oxychloride with potassium dihydrogen phosphate under all conditions tested produces a phase that is completely different from the intercalate prepared by ion exchange, which corresponds to $KZrH(PO_4)_2{\cdot}xH_2O$ (JCPDS no. 00-033-1069). With the exception of syntheses at P/Zr = 2 and 3 and temperatures of 140 and 160 °C, where kosnarite $KZr_2(PO_4)_3$ is formed, the products are probably an α-type structure, as it follows from comparison with the standard α-$KHZr(PO_4)_2$ (JCPDS no. 04-012-8202) as can be seen in Fig. 3 and S6 in SI. The crystallinity of these phase is not significantly affected by either the P/Zr ratio or the reaction temperature. Similarly as in the previous cases, the potassium intercalates prepared by minimal liquid method consist of agglomerates of particles with a non-specific shape (see Fig. S5 in SI).

As evidenced by the PXRD patterns presented above, variations in the P/Zr molar ratio and reaction temperature do not alter the phase composition of the synthesized product except for $NaZr_2(PO_4)_3$ and $KZr_2(PO_4)_3$ formed at low P/Zr ratios. However, these parameters significantly influence the crystallinity and crystallite size of the resulting material. Experimental results indicate that conducting the synthesis at a P/Zr ratio of 4 and a temperature of 120 °C yields products with adequate crystallinity, while avoiding the formation of unwanted compounds and the additional costs associated with higher reagent excess and elevated temperatures. Therefore, all other syntheses described below are carried out under these conditions.

Influence of zirconium source

In addition to the commonly used zirconium oxychloride and zirconium propoxide, zirconium oxynitrate and zirconium sulfate were also used as zirconium sources. As seen from Fig. 4, the zirconium compound used has a significant influence on the composition and crystallinity of the resulting product. When using propoxide, the products were amorphous for all three cations.

Reaction of oxychloride or oxynitrate with ammonium and sodium dihydrogen phosphates leads to products with a γ-structure. While the reaction of potassium dihydrogen phosphate with oxychloride produces a very well-crystalline product with an α-structure, the reaction with oxynitrate produced a product with a very low degree of crystallinity, so the type of structure cannot be determined based on PXRD patterns.

Reactions involving zirconium sulfate produced a γ-type structure only in the presence of ammonium cations, accompanied by a minor α-ZrP phase. For sodium cations, the formation of predominantly α-ZrP is favorable. Interestingly, the reaction of zirconium sulfate with potassium dihydrogen phosphate yielded a product with a diffraction pattern distinct from both α-ZrP and α-$KHZr(PO_4)_2$, indicating the possible formation of a novel or mixed-phase material. The different products formed during the reaction of different zirconium compounds could be related to the fact that part of the cations from the respective dihydrogen phosphates are bound to anions originating from the zirconium compound forming corresponding chloride, nitrate or sulfate as by-products.

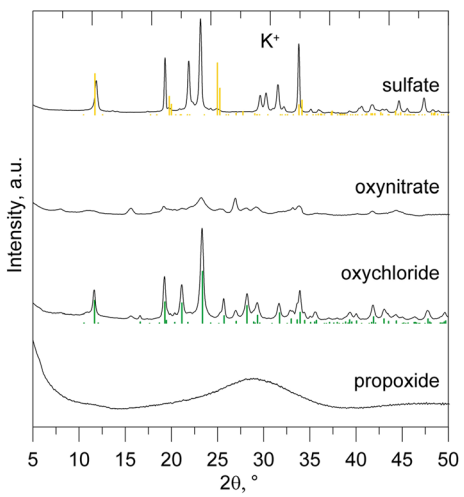

Fig. 3 Powder X-ray diffraction patterns of potassium intercalates prepared at various P/Zr ratios and temperatures and by ionic exchange from γ-ZrP. Light green lines corresponds to $KZrH(PO_4)_2{\cdot}xH_2O$ (JCPDS no. 00-033-1069) and green to $KZrH(PO_4)_2$ (JCPDS no. 04-012-8202).

Effect of metal/hydrogen ratio

To elucidate the influence of cation concentration on the structural characteristics of the resulting zirconium phosphate phases, a series of reactions was conducted using zirconium oxychloride and zirconium propoxide as precursors. The reactions followed the general stoichiometry:

$$ZrOCl_2 + xMH_2PO_4 + (4-x)\ H_3PO_4 \rightarrow M_yH_{(2-y)}Zr(PO_4)_2 \cdot nH_2O$$

$$Zr(OC_3H_7)_4 + xMH_2PO_4 + (4-x)H_3PO_4 \rightarrow M_yH_{(2-y)}Zr(PO_4)_2 \cdot nH_2O.$$

In all reactions, P/Zr molar ratio was maintained at 4. The variable x represents the molar proportion of the monovalent cation source (MH_2PO_4), and its decrease corresponds to a reduction in the cation content in the reaction mixture. All syntheses were performed at 120 °C.

Ammonium intercalates. The use of zirconium oxychloride led to the formation of a mixed-phase product comprising α-zirconium phosphate (α-ZrP, indicated in yellow) and ammonium-intercalated γ-zirconium phosphate (γ-ZrP, indicated in red), even at low additions of H_3PO_4, as illustrated in Fig. 5. For values of $x \leq 2$, the product consisted exclusively of α-ZrP. In contrast, reactions employing zirconium propoxide yielded a pure γ-phase up to x = 1.5, while pure α-ZrP was obtained at x = 0.5.

The compositions of all monophasic ammonium-intercalated products are given in Table S3 of SI. EDX analysis confirmed that the P/Zr molar ratio remained close to 2 across all

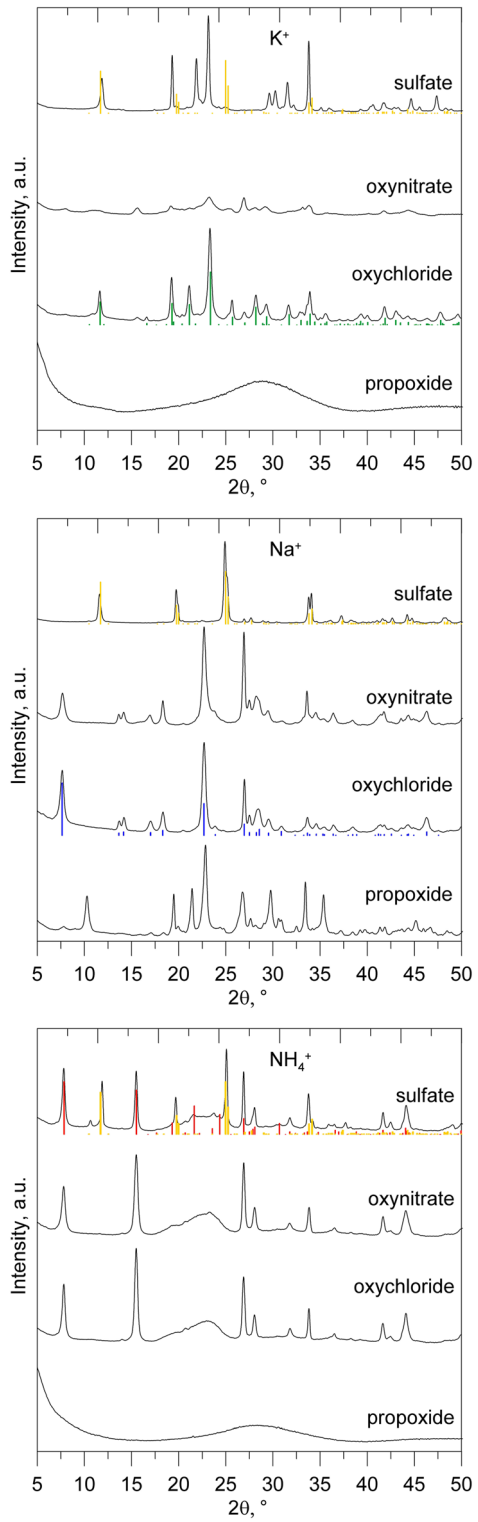

Fig. 4 PXRD patterns of NH_4, Na and K intercalates prepared from various zirconium sources. The red lines correspond to γ-$H(NH_4)Zr(PO_4)_2$ (JCPDS no. 00-033-0842), the blue ones to indexed pattern of $NaHZr(PO_4)(HPO_4)\cdot 1.4H_2O$, the green ones to $KZrH(PO_4)_2$ (JCPDS no. 04-012-8202) and the yellow ones to α-ZrP (JCPDS no. 04-010-6268).

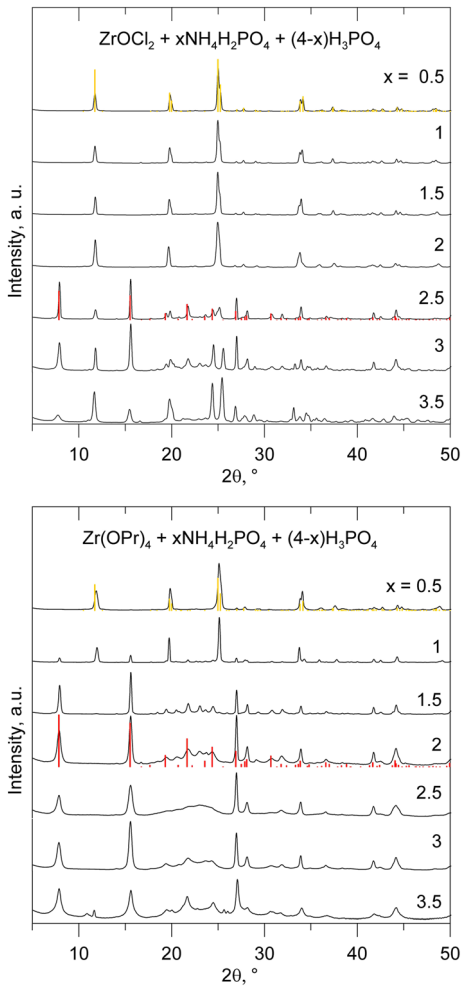

Fig. 5 PXRD patterns of NH_4 intercalates prepared from zirconium chloride and propoxide with a mixture of ammonium dihydrogen phosphate and phosphoric acid. The red lines correspond to γ-$H(NH_4)Zr(PO_4)_2$ (JCPDS no. 00-033-0842), and the yellow ones to α-ZrP (JCPDS no. 04-010-6268).

samples. The nitrogen content was consistent with the empirical formula $(NH_4)HZr(PO_4)(HPO_4)$ for samples with $x \leq 2$. For the sample with $x = 1.5$, a slight reduction in nitrogen content was observed, corresponding to the formula $(NH_4)_{0.9}H_{0.1}Zr(PO_4)(HPO_4)$. All ammonium intercalates are anhydrous. The particle morphology of these ammonium intercalates closely resembles that of those synthesized only from ammonium dihydrogen phosphate and exhibits negligible variation with changes in x as illustrated in Fig. S7 in SI.

To verify the formation of either the α- or γ-phase of zirconium phosphate (ZrP), selected samples underwent ion exchange in a 1 M hydrochloric acid solution. PXRD patterns of the exchanged samples are shown in Fig. S8 in the SI. As expected, samples prepared from propoxide with $x = 2$ and 1.5 were fully converted to γ-ZrP, ion exchange of the sample prepared from oxychloride with $x = 3$ yielded a mixture of α- and γ-ZrP.

To complement the XRD analysis, ^{31}P MAS NMR measurements have been performed (Fig. 6). The samples with x =

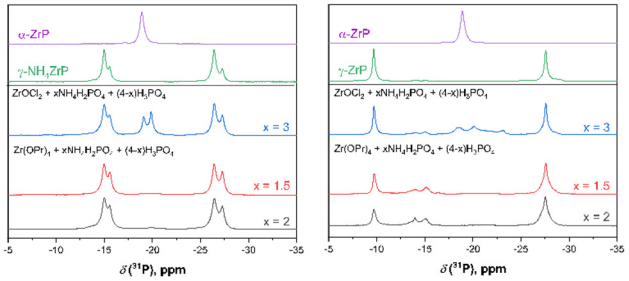

Fig. 6 Left – ^{31}P MAS NMR spectra of NH_4 intercalates prepared from zirconium oxychloride and propoxide with a mixture of ammonium dihydrogen phosphate and phosphoric acid. Right – ^{31}P MAS NMR spectra of the same samples after ion exchange in a 1 M hydrochloric acid solution. ^{31}P MAS NMR spectra of α-, γ-ZrP and γ-NH_4ZrP phases are shown above for clarity.

1.5–2 contain pure γ-$(NH_4)HZr(PO_4)(HPO_4)$ as can be seen from the comparison with the spectrum of a sample prepared by the classical method.[20] On the other hand, the sample with x = 3 contains a considerable amount of α-phase. The ammonium-intercalated products are seen as doublets of the lines attributed to α- or γ-ZrP phases, at −19 ppm for α-ZrP and −15, 26 ppm for γ-ZrP. To prove this, for the sample x = 3 the ^{31}P–^{31}P 1Q–2Q spectrum was measured (shown in Fig. S9 in SI). It confirmed that doublets arise from species that are in close vicinity to each other because of the presence of cross peaks.

After the ion exchange in a 1 M hydrochloric acid solution, the resulting ^{31}P MAS NMR spectra show that most of the samples are transformed into γ-ZrP phase with traces of ammonium intercalates.

Sodium intercalates. Similarly, in the reactions involving sodium dihydrogen phosphate and zirconium oxychloride, a biphasic product containing α-zirconium phosphate (α-ZrP) is formed even at the lowest additions of H_3PO_4, as shown in Fig. 7. In contrast, when zirconium propoxide is used as the precursor, sodium-intercalated γ-zirconium phosphate (indicated in blue) is observed for $x \geq 2$. The XRPD pattern of the sample with x = 1.5 exhibits significant deviations—particularly in the 2θ range of 10–20°— from those of the γ-phase, although no evidence of α-ZrP formation is detected. At lower values of x, the presence of α-ZrP becomes apparent in the product. Similarly as it was in the case of ammonium intercalates, the particle shape of sodium intercalates is not significantly affected by changing x as can be seen from Fig. S7 in SI.

As presented in Table S3 of the SI, the sodium content in the synthesized products systematically decreases with decreasing values of x, ranging from a Na/Zr molar ratio of 1.4 at x = 3.5 to a ratio of 1.0 at x = 2.0. For the sample with x = 1.5, which exhibits PXRD patterns distinct from those of the ion-exchanged counterpart, the Na/Zr ratio falls below 1.0. All sodium-intercalated phases contain co-intercalated water molecules within the interlayer galleries, with the water content varying between 1.0 and 1.5 molecules per formula unit.

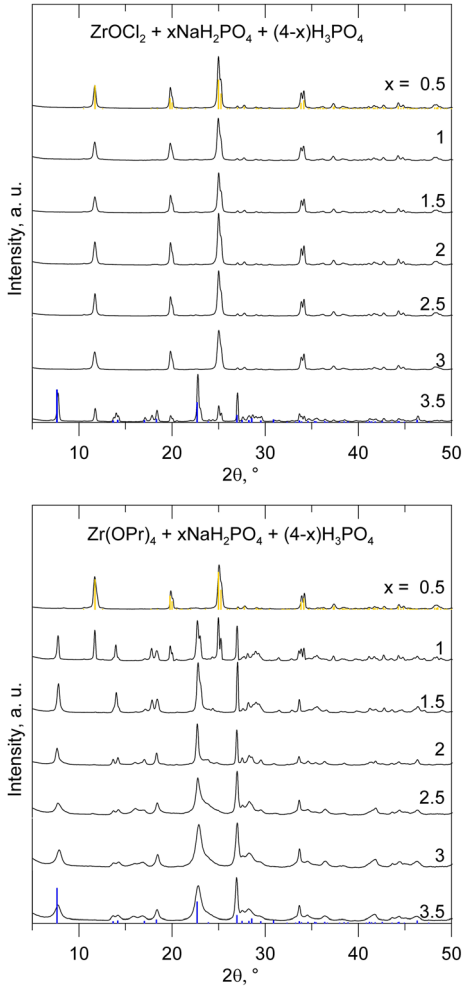

Fig. 7 PXRD patterns of sodium intercalates prepared from zirconium chloride or propoxide with a mixture of sodium dihydrogen phosphate and phosphoric acid. The blue lines to indexed pattern of $NaHZr(PO_4)(HPO_4)\cdot 1.4H_2O$ and the yellow ones to α-ZrP (JCPDS no. 04-010-6268).

According to Fig. S10 in the SI, treatment with 1 M HCl results in the transformation of the samples with x = 2.0 and x = 1.5 into the γ-ZrP phase, which confirms the formation of an intercalate with a γ-structure in both cases. In contrast, the sample with x = 1.0 yields a biphasic product comprising both α-ZrP and γ-ZrP.

^{31}P MAS NMR analysis confirmed the formation of complex sodium-intercalated ZrP structures (Fig. 8). For samples with x = 1.5–2, the dominant phase is a complex form of γ-structure, characterized by a broad and intricate ^{31}P NMR lineshape. This complexity arises from the presence of multiple intercalate configurations within the material. To support this interpretation, ^{23}Na MAS NMR and ^{23}Na MQMAS measurements were conducted. These revealed several distinct ^{23}Na chemical environments, indicating a heterogeneous distribution of sodium ions (see Fig. S11 in the SI). At x = 3, the sample consists of both Na-intercalated γ-ZrP and a predominantly pure α-ZrP phase.

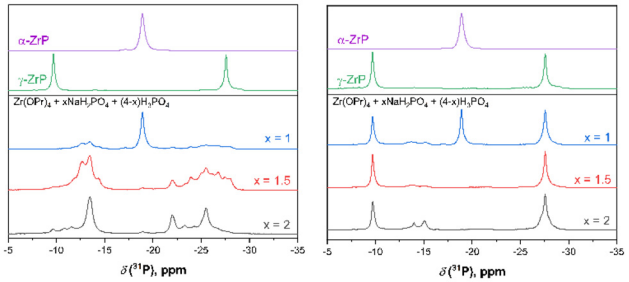

Fig. 8 Left – ^{31}P MAS NMR spectra of sodium intercalates prepared from zirconium propoxide with a mixture of sodium dihydrogen phosphate and phosphoric acid. Right – ^{31}P MAS NMR spectra of the same samples after ion exchange in a 1 M hydrochloric acid solution. ^{31}P MAS NMR spectra of α- and γ-ZrP phases are shown above for clarity.

After the ion exchange in a 1 M hydrochloric acid solution, the resulting ^{31}P MAS NMR spectra show that Na intercalated γ-ZrP phase is transformed into pure γ-ZrP phase with traces of sodium intercalates.

Potassium intercalates. Neither zirconium oxychloride nor propoxide reaction with potassium dihydrogen phosphate forms a crystalline γ-structure (see Fig. 9). In the case of propoxide, samples with x = 3.5 and 3 are amorphous, while samples with x = 2.5 and 2 form potassium intercalated α-ZrP (marked with green). The PXRD patterns of samples with x = 1.5 and 1 differ slightly from the previous ones, and the same phase is formed in the reaction of oxychloride at x = 3.5 and 3 or in the reaction of zirconium sulfate with potassium dihydrogen phosphate (see Fig. 4). In the reaction of oxychloride with x = 2 and lower, only α-ZrP is formed, and at x = 2.5 a mixture of both phases is formed.

As shown in Table S3 of the SI, the K/Zr molar ratio decreases progressively with decreasing values of x, ranging from 1.8 at x = 3.0 to 1.2 at x = 2.0. Samples exhibiting PXRD patterns that deviate from the reference structure of KZrH$(PO_4)_2$ possess K/Zr ratios below 1.0. Additionally, potassium intercalates synthesized from zirconium oxychloride with x = 3.5 and 3.0, having the same diffraction pattern, exhibit K/Zr ratios of 0.9 and 0.8, respectively. All potassium intercalates are anhydrous.

The powder diffraction patterns of $K_{0.9}H_{1.1}Zr(PO_4)_2$ and $K_{0.8}H_{1.2}Zr(PO_4)_2$ (from propoxide, x = 1 and 1.5, respectively) can be indexed in the monoclinic system (SI Tables S4, S5 and Fig. S12, S13). For both samples, the lattice parameters $a \approx$ 9.20 Å and $b \approx$ 5.30 Å are obtained. This means that the lattice parameters in the layer direction are practically identical to the values given for the standard KHZr$(PO_4)_2$ (9.22 and 5.32 Å) and the layer structure is preserved. The values for the parameter c and the angle β are different, which means that the way the layers are stacked and the arrangement of potassium ions between the layers are different. Also, the probable space group $P2_1/a$ differs from $P2/c$ given for KHZr$(PO_4)_2$ (JCPDS 04-012-8202). In Fig. S12 and S13, it can be observed that the (hk0) diffractions have a clearly smaller width (FWHM ~ 0.25) than the(00l) and (hkl) diffractions (FWHM ~ 0.39). This also

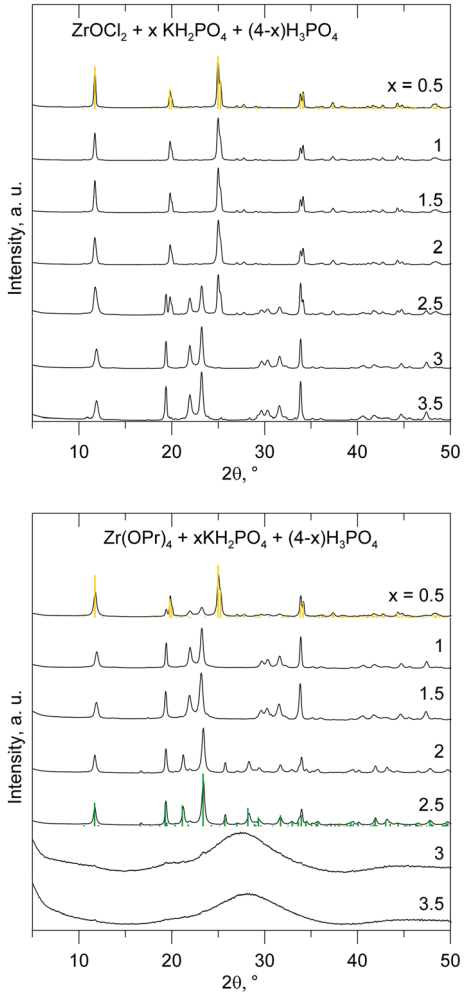

Fig. 9 PXRD patterns of potassium intercalates prepared from zirconium chloride or propoxide with a mixture of potassium dihydrogen phosphate and phosphoric acid. The green lines correspond to KZrH$(PO_4)_2$ (JCPDS no. 04-012-8202) and the yellow ones to α-ZrP (JCPDS no. 04-010-6268).

indicates that the layer in the ab plane is very well ordered, while the order in the c direction is worse.

PXRD patterns of the samples exchanged in 1 M HCl are shown in Fig. S14 in the SI. The amorphous potassium intercalate prepared from zirconium propoxide at x = 3.5 remained amorphous after acidic treatment. All other potassium intercalates, irrespective of their initial PXRD patterns, underwent transformation to the α-ZrP phase upon acid treatment.

^{31}P MAS NMR analysis confirms that when potassium dihydrogen phosphate is used, the only phase formed is α-structure (see Fig. 10). However, at specific x values—namely x = 2.5 for the $ZrOCl_2$ route and x = 1.5 for the $Zr(OPr)_4$ route—the spectra reveal signs of potassium intercalation. This is evidenced by the appearance of additional spectral lines. To investigate these new features, ^{31}P–^{31}P 1Q–2Q NMR measurements were performed (Fig. S15 in the SI). The strong correlations observed between all peaks in the 2D spectrum indicate

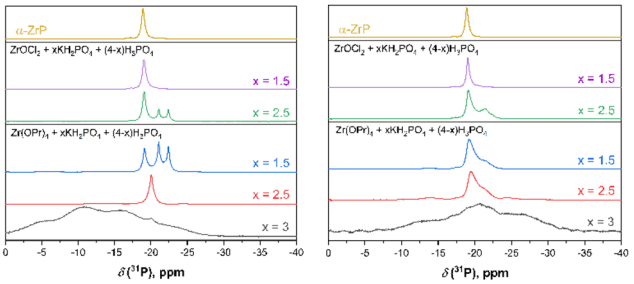

Fig. 10 Left – ^{31}P MAS NMR spectra of potassium intercalates prepared from zirconium oxychloride or propoxide with a mixture of potassium dihydrogen phosphate and phosphoric acid. Right – ^{31}P MAS NMR spectra of the same samples after ion exchange in a 1 M hydrochloric acid solution. ^{31}P MAS NMR spectra of α-ZrP are shown above for clarity.

that these signals originate from species in close proximity, confirming that potassium ions are intercalated within the α-ZrP structure. Similarly, as it was seen in the PXRD data, when x = 3 in the $Zr(OPr)_4$ route, the structures formed possess poor crystallinity, which results in very broad ^{31}P MAS NMR linewidths.

After the ion exchange in a 1 M hydrochloric acid solution, the resulting ^{31}P MAS NMR spectra show that α-potassium intercalated ZrP phase is transformed into α-ZrP phase with traces of potassium intercalates.

Conclusions

Zirconium hydrogen phosphates intercalated with ammonium, *via* a minimal liquid-assisted approach, involving the reaction of a zirconium precursor with the corresponding metal dihydrogen phosphate. Samples obtained solely through mechanical grinding were amorphous; however, subsequent thermal treatment at 120 °C or 180 °C resulted in the formation of crystalline products. The degree of crystallinity increased with both the P/Zr molar ratio in the starting mixture and the reaction temperature, although these parameters did not affect the phase composition of the final products.

The formation of α- or γ-type zirconium phosphate structures was found to depend on both the intercalating cation and the zirconium source. Specifically, potassium dihydrogen phosphate consistently yielded compounds with α-structure, whereas ammonium and sodium dihydrogen phosphates led to either α- or γ-modification, depending on the reaction conditions. To identify the conditions favoring γ-phase formation, a series of reactions was performed using zirconium propoxide and mixtures of dihydrogen phosphate and phosphoric acid at varying molar ratios. While reactions with pure dihydrogen phosphate produced amorphous materials, γ-intercalates were obtained within a dihydrogen phosphate/phosphoric acid molar ratio range of 3.5/0.5 to 1.5/2.5. Lower ratios resulted in either mixed γ/α phases or pure α-ZrP.

The presence of α- or γ-type intercalates was confirmed through hydrochloric acid treatment, which selectively yielded α- or γ-ZrP, and further validated by solid-state ^{31}P NMR spectroscopy.

Conflicts of interest

There are no conflicts to declare.

Data availability

The data supporting this article have been included as part of the supplementary information (SI). Supplementary information: characterization data, SEM images, indexed powder diffraction patterns, powder diffraction patterns of HCl treated samples, ^{31}P–^{31}P 1Q–2Q NMR spectra, ^{23}Na MQMAS NMR spectrum. See DOI: https://doi.org/10.1039/d5dt02548f.

Acknowledgements

The authors (K. M., L. B., and J. S.) acknowledge financial support from the Ministry of Education, Youth and Sports of the Czech Republic (grant no. LM2023037). R. L. and V. K. acknowledge funding from the Research Council of Lithuania (LMTLT) under project no. S-MIP-23-47. Additionally, R. L. and V. K. thank the Center for Spectroscopic Characterization of Materials and Electronic/Molecular Processes (SPECTROVERSUM Infrastructure) for access to NMR instrumentation.

References

1 H. P. Xiao and S. H. Liu, *Mater. Des.*, 2018, **155**, 19–35.
2 C. Bisio, J. Brendlé, S. Cahen, Y. J. Feng, S. J. Hwang, K. Melanova, M. Nocchetti, D. O'Hare, P. Rabu and F. Leroux, *Dalton Trans.*, 2024, **53**, 14525–14550.
3 C. Bisio, J. Brendlé, S. Cahen, Y. J. Feng, S. J. Hwang, M. Nocchetti, D. O'Hare, P. Rabu, K. Melanova and F. Leroux, *Dalton Trans.*, 2024, **53**, 14551–14581.
4 A. Bashir, S. Ahad, L. A. Malik, A. Qureashi, T. Manzoor, G. N. Dar and A. H. Pandith, *Ind. Eng. Chem. Res.*, 2020, **59**, 22353–22397.
5 M. Pica, A. Donnadio and M. Casciola, *Coord. Chem. Rev.*, 2018, **374**, 218–235.
6 A. Clearfield and J. A. Stynes, *J. Inorg. Nucl. Chem.*, 1964, **26**, 117–129.
7 C. Trobajo, S. A. Khainakov, A. Espina and J. R. Garcia, *Chem. Mater.*, 2000, **12**, 1787–1790.
8 G. Alberti and E. Torraca, *J. Inorg. Nucl. Chem.*, 1968, **30**, 317–318.
9 D. Capitani, M. Casciola, A. Donnadio and R. Vivani, *Inorg. Chem.*, 2010, **49**, 9409–9415.
10 J. F. Yu, H. Ding, J. Lampron, B. R. Martin, A. Clearfield and L. Y. Sun, *Inorg. Chem.*, 2020, **59**, 1204–1210.

11 L. Y. Sun, W. J. Boo, H. J. Sue and A. Clearfield, *New J. Chem.*, 2007, **31**, 39–43.
12 M. Shuai, A. F. Mejia, Y. W. Chang and Z. D. Cheng, *CrystEngComm*, 2013, **15**, 1970–1977.
13 H. Benhamza, P. Barboux, A. Bouhaouss, F. A. Josien and J. Livage, *J. Mater. Chem.*, 1991, **1**, 681–684.
14 W. J. Mu, Q. H. Yu, R. Zhang, X. L. Li, R. Hu, Y. He, H. Y. Wei, Y. Jian and Y. C. Yang, *J. Mater. Chem. A*, 2017, **5**, 24388–24395.
15 S. Bevara, P. Giri, S. J. Patwe, S. N. Achary, R. K. Mishra, A. Kumar, A. K. Sinha, C. P. Kaushik and A. K. Tyagi, *J. Environ. Chem. Eng.*, 2018, **6**, 2248–2261.
16 Y. Cheng, X. D. Wang, S. Jaenicke and G. K. Chuah, *ChemSusChem*, 2017, **10**, 3235–3242.
17 Y. Cheng, S. S. Y. Chui, X. D. T. Wang, S. Jaenicke and G. K. Chuah, *Inorg. Chem.*, 2019, **58**, 13020–13029.
18 Y. Cheng, H. W. Zhang, J. A. Jaenicke, E. C. P. Tan and G. K. Chuah, *ACS Sustainable Chem. Eng.*, 2019, **7**, 895–904.
19 Y. Cheng, X. D. Wang, S. Jaenicke and G. K. Chuah, *Inorg. Chem.*, 2018, **57**, 4370–4378.
20 D. M. Poojary, B. Shpeizer and A. Clearfield, *J. Chem. Soc., Dalton Trans.*, 1995, 111–113.
21 *Database PDF-5+, Joint Committee on Powder Diffraction Standards*, International Centre of Diffraction Data, Swarthmore, PA, 2025.
22 R. Shirley, *The crysfire 2002 system for automatic powder indexing: user's manual*, The Lattice Press, 41 Guildford Park Avenue, Guildford, Surrey GU2 7NL, England, 2002.
23 A. Le Bail, H. Duroy and J. L. Fourquet, *Mater. Res. Bull.*, 1988, **23**, 447–452.
24 Y. Zhu, G. Hasegawa, K. Kanamori, T. Kiyomura, H. Kurata, K. Hayashi and K. Nakanishi, *CrystEngComm*, 2017, **19**, 4551–4560.